ESTIMATION OF THE R - CURVE BY IN - SITU MEASUREMENTS

E. Schick*, J. Ude*, F. Michel* and H. Blumenauer*

The micromechanisms of ductile fracture was examined using an in-situ electron microscopy technique. The investigations allow the direct observation of the deformation process near the crack tip and the contineous measurement of CTOD on the surface of the specimen during loading. Therefore this method was used to evaluate microcrack resistance curves of the steels 17CrMoV10 and X6CrNiTi1810 with different microstructure. The curves are discussed in connection with sets of micrographs of the crack tip region at increasing load levels.

INTRODUCTION

In order to make progress in the relationship between the microstructure and the elastic-plastic fracture mechanics parameter detailed knowledge on the mechanisms of ductile fracture is needed. The direct experimental evidence of the highly localized damage phenomenon at the crack tip is possible using an in-situ fracture mechanics testing in the SEM (Wilsdorf (1), Stephens (2), Sohn (3) and Luo (4)). In this case the microcrack resistance curve can be estimated in connection with monitoring the damage process at the crack tip. Especially the crack tip blunting (stretch zone formation), followed by microvoid nucleation and coalescence as the critical strain controlled stages of ductile fracture, can be correlated to the microstructure simultaneously, and therefore better physical interpretations of the crack initiation point and the CTOA are possible.

EXPERIMENTAL PROCEDURE

Investigations were carried out on the low-alloyed pressure vessel steel 17CrMoV10 with two kinds of bainitic microstructure and the austenitic steel

* Otto-von-Guericke-University Magdeburg, Germany

X6CrNiTi1810. The chemical composition, heat treatment, microstructure and mechanical properties are given in the tables 1 and 2.

TABLE 1 - Chemical composition [%]

Material	C	Si	Mn	P	S	Cr	Ni	Mo	V	Ti
17CrMoV10	0.17	0.34	0.45	0.014	0.010	2.71	<0.1	0.24	0.12	<0.01
X6CrNiTi1810	0.07	0.57	1.07	0.022	0.005	17.09	8.88	0.14	<0.1	0.38

TABLE 2 - Heat treatment, microstructure and mechanical properties

Material	State	Microstructure	R_e [MPa]	R_m [MPa]
17CrMoV10 (V1)	quenched and tempered: 950°C/1h/oil/ 650°C/7 h/air	tempered bainite, with rodlike carbides $(Cr,Fe)_{23}C_6$ (shape factor 0.4 -0.7); VC neadles (5 x 22 nm)	518	647
17CrMoV10 (V2)	as V1 + 680°C/ 160 h/air	tempered bainite; larger,but fewer carbides $(Cr,Fe)_{23}C_6$ (shape factor 0.8 - 1); VC neadles (40 x 12 nm)	368	548
X6CrNiTi1810	quenched from 1050 °C, water	austenite, Ti-nitrides ($\leq$ 10 µm) and Ti-carbo-nitrides (< 1µm)	240	620

Charpy specimens were pre-cracked by fatigue and than machined to small tensile specimens (thickness $\approx$ 2 mm; ligament length $\approx$3 mm, $a_o/W \approx 0.5$). For the in-situ CTOD measurement the position at the initial fatigue crack tip was marked by microhardness indentations. The specimens were loaded by a strain rate of 0.5µm/s. In addition a.c. potential drop technique was applied to monitor the crack initiation point.

RESULTS AND DISCUSSION

The obtained microcrack resistance curves are plotted in fig.1, and the crack initiation points estimated by stretch zone and potential drop measurements are marked by arrows. It is obvious that the bainitic steel has a higher crack resistance in terms of CTOD against crack growth than the austenitic steel. Fig.2 illustrates the influence of the bainitic microstructure on the damage process at the crack tip. At first the crack blunts at the lower part of the fatigue crack.

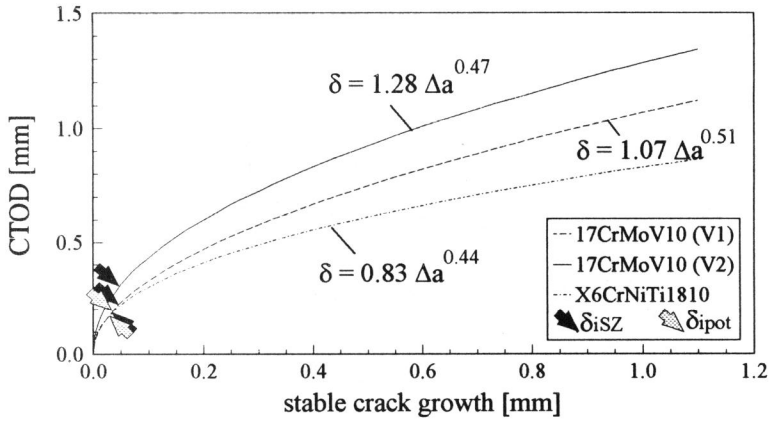

Figure 1 Microcrack resistance curves

During increasing load the crack tip is rounded off at the corners, whereas the grains in front of the crack are extended to several times of theirs original length. Small shear bands are visible as a bright zone in the upper and lower part of the squarely blunted crack. Fig. 2d demonstrates that the new crack nuclei appearing in the vertical crack front (2c) was removed by deformation in lateral direction. In the grains with highly concentrated deformation two microcracks are originated along the shear bands under $\approx 45°$ leading to a zig-zag crack extension. Accompanying a part of the fatigue crack surface close to the crack tip is transferred into the stretched zone, what means, that a certain amount of the fatigue crack is moving backwards during the blunting process (marked by pairs of arrows in the vicinity of the crack tip). This fact has been taken into account in order to define the location for CTOD or crack extension measurements accurately.

For the steel X6CrNiTi1810 (fig.3) the blunting process provides a smoothly rounded crack tip, and the crack extension starts after intense sliding only in the midsection of the specimen without crack branching or zig-zag- pathes.
Therefore it can be concluded, that the characteristic zig-zag crack path in the bainitic microstructure is caused by the influence of the carbides as second order population. Fig. 4 shows the void nucleation at carbides, and during the in-situ experiments could be observed, that the microcrack joins these voids, whereby the carbides stabilize the microstructure against rather crack growth.

In the long-time annealed condition V2 the sulfides (first order population) are not changed by the heat treatment, but the carbides are larger and more globular.

Additional a higher work hardening exponent results from a substructure with dislocations rearranged into lower energy configurations by formation of a subgrain structure with low-angle boundaries. These two factors promote higher CTOD values in comparison to the microstructure V1.

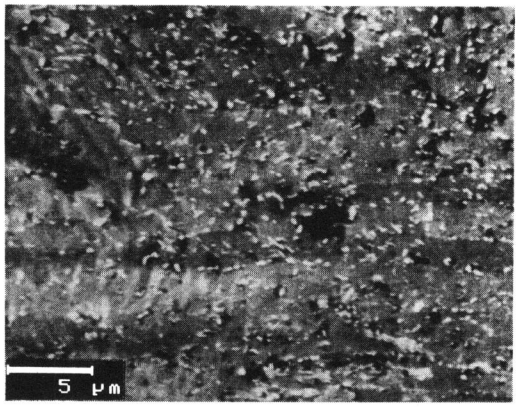

Figure 4 Nucleation of voids at carbides (17CrMoV10/V1)

The investigations have demonstrated, that in-situ measurements are very successful to study the interaction between a complicated microstructure and the damage process at the crack tip.

ACKNOWLEDGEMENT

This work was supported by Deutsche Forschungsgemeinschaft Bonn.

REFERENCES

(1) Wilsdorf, H.G., Z. Metallkde. 75, 1985, Nr. 2, S. 154 - 160

(2) Steffens, R.R., Grabowski, L. and Hoeppner, D.W., Intern. J. Fatig. Vol. 15, 1993, pp. 273 - 282

(3) Sohn, K.S., Lee, S. and Kim, N.J., Mat.Science and Engng., A 163, 1993, pp. 11 - 21

(4) Luo, L.G., Quarrington, A.I. and Embury, J.D., Engng. Fract. Mech., Vol.31, 1988, No. 2, pp. 349 - 356

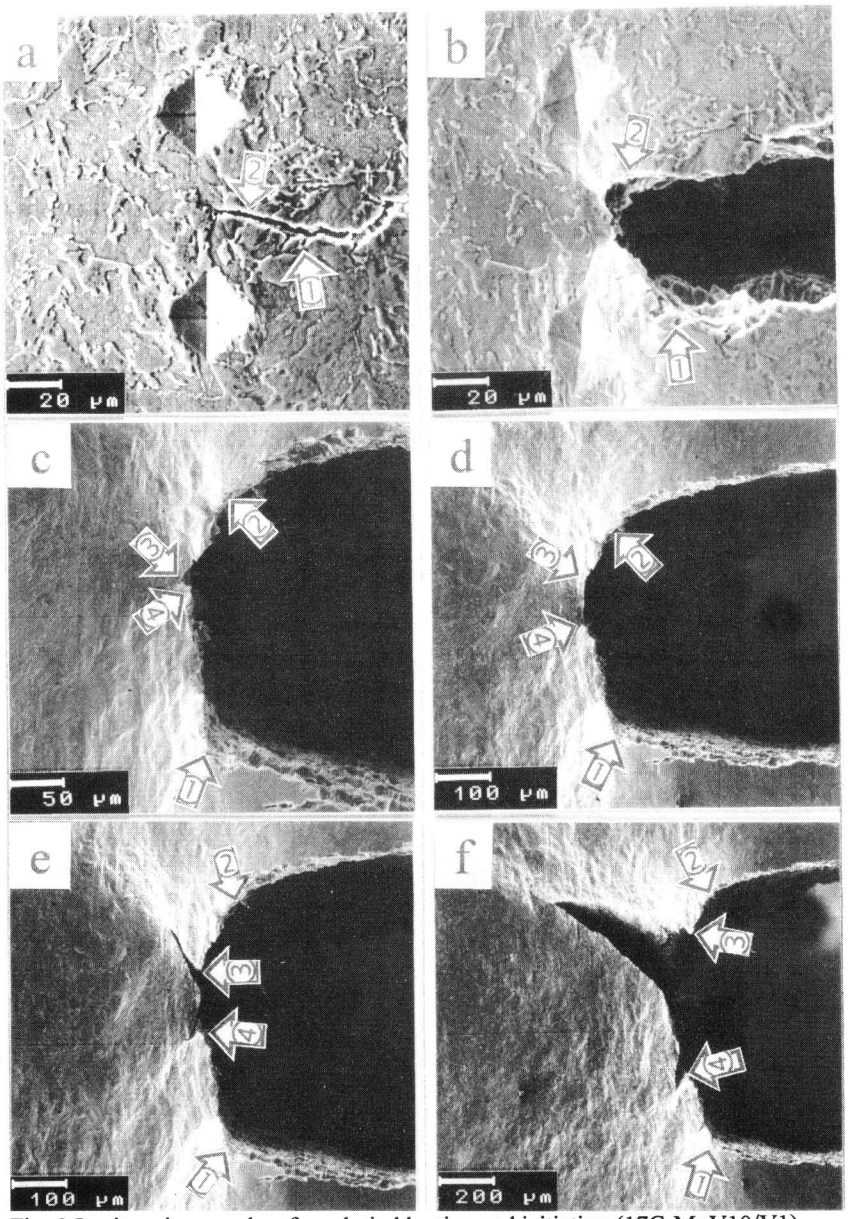

Fig. 2 In-situ micrographs of crack tip blunting and initiation (17CrMoV10/V1)

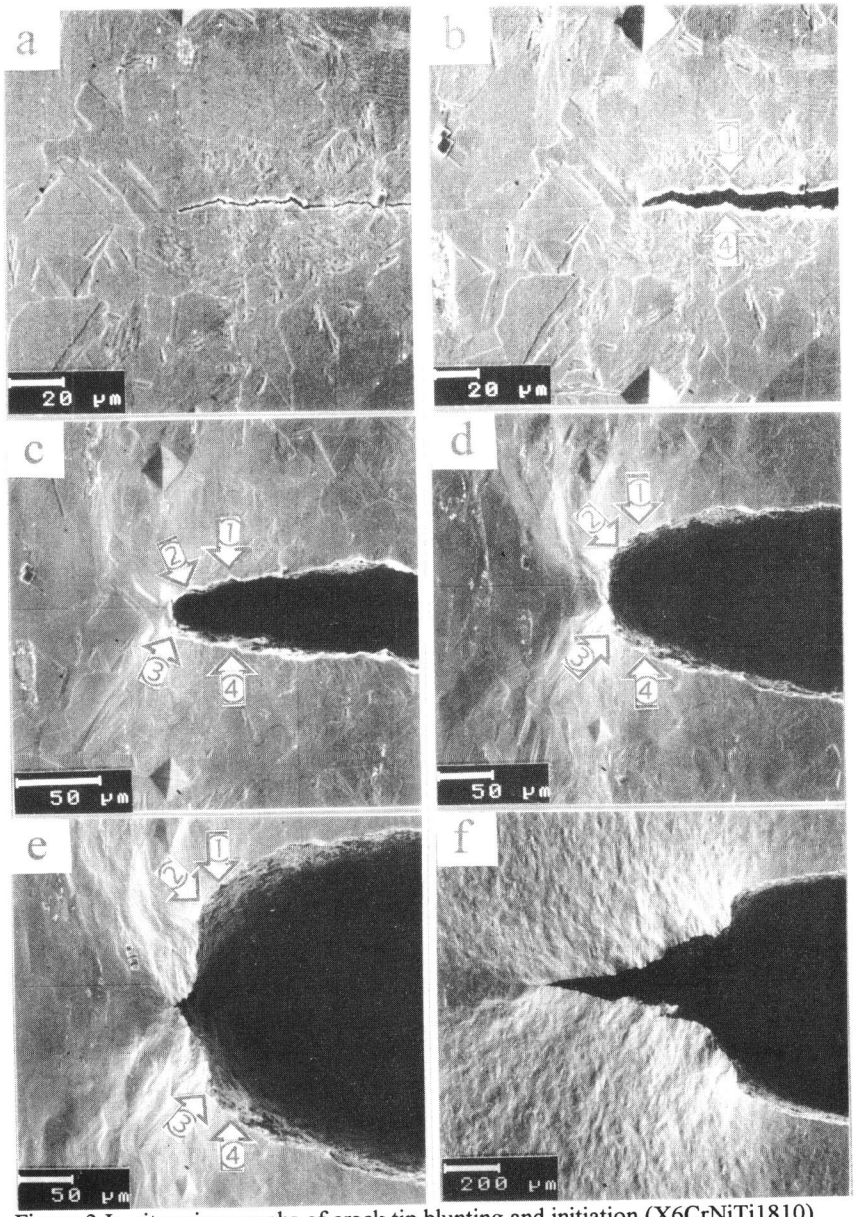

Figure 3 In-situ micrographs of crack tip blunting and initiation (X6CrNiTi1810)